

**Impacts of socio-economic and climate changes
on water, food, bioenergy, land use, and ecosystems**

T. Yokohata^{1*}, T. Kinoshita², G. Sakurai³, S. Fujimori⁴, A. Ito¹, Y. Satoh¹, Y. Pokhrel⁵, E. Kato⁶,
M. Okada⁷, K. Tachiiri^{8,1}, K. Matsumoto^{9,8}, S. Emori¹, and K. Takahashi¹⁰

1 Earth System Division, National Institute for Environmental Studies, Tsukuba, Japan

2 College of Agriculture, Ibaraki University, Ami, Japan

3 Institute for Agro-Environmental Sciences, National Agriculture and Food Research Organization, Tsukuba,
Japan

4 Graduate School of Engineering, Kyoto University, Kyoto, Japan

5 Department of Civil and Environmental Engineering, Michigan State University, Michigan, USA

6 Institute of Applied Energy, Tokyo, Japan

7 Climate Change Adaptation Center, National Institute for Environmental Studies, Tsukuba, Japan

8 Research Institute for Global Change, Japan Agency for Marine-Earth Science and Technology, Yokohama,
Japan

9 Faculty of Economics, Toyo University, Tokyo, Japan

10 Social System Division, National Institute for Environmental Studies, Tsukuba, Japan

Contents of this file

Text S1

Captions for Tables S1

Figure S1 to S8

Additional Supporting Information (Files uploaded separately)

Tables S1

Text S1. The impacts of climate and CO2 on food crop yields and cropland area

As shown in Figure 8, the absolute impacts of climate and CO2 on food crop yields are similar, but their impacts on food cropland areas are different. This is because the food cropland area is generally inversely proportional to the food crop yields. Let Y_0 be the crop yield of the CL+FE experiment, $Y_0 + Y_{CL}$ be the crop yield of the noCL+FE experiment, and $Y_0 - Y_{FE}$ be the crop yield of the CL+noFE experiment. Here, Y_{CL} and Y_{FE} represent the contributions of the climate change and the CO₂ fertilization effect on the crop yield, respectively (both positive values). Assuming that the food cropland areas of the CL+FE, noCL+FE, and CL+noFE experiments are A_0 , A_{CL} , and A_{FE} , respectively, then the ratio of each cropland area is as follows.

$$A_{CL}/A_0 \sim Y_0/(Y_0 + Y_{CL}) = (1 + Y_{CL}/Y_0)^{-1}$$

$$A_{FE}/A_0 \sim Y_0/(Y_0 - Y_{FE}) = (1 - Y_{FE}/Y_0)^{-1}$$

If the contributions of climate change and the CO₂ fertilization effects are very small (Y_{CL}/Y_0 , Y_{FE}/Y_0 approach to zero),

$$A_{CL}/A_0 \sim 1,$$

$$A_{FE}/A_0 \sim 1.$$

On the other hand, if the contributions of climate change and the CO₂ fertilization effect are large enough, that is, if Y_{CL}/Y_0 and Y_{FE}/Y_0 approach to 1, then

$$A_{CL}/A_0 \rightarrow 1/2,$$

$$A_{FE}/A_0 \rightarrow \infty.$$

Therefore, the contribution of CO₂ fertilization effects on food cropland area (A_{FE}) is relatively large compared to that of climate change (A_{CL}). For example, if the food crop yields in 2100 under the RCP8.5 scenario are $Y_0 = 5.5$, $Y_{CL} = 4.0$, $Y_{FE} = 3.0$ [t/ha], then the changes in food cropland area can be estimated as $A_{CL}/A_0 \sim 0.57$ and $A_{FE}/A_0 \sim 2.2$ by using the above equations. This estimation corresponds to a decrease in A_{CL} by approximately 43%, A_{FE} increases by approximately 120%, which is generally consistent with the results shown in Figure 9. In other words, even if the climate and CO₂ impacts

on crop yields (Y_{CL} and Y_{FE}) are comparable, their effects on changes in cropland areas ($A_{CL}-A_0$ and $A_{FE}-A_0$) are relatively larger in the latter case compared to the former case.

Table S1. The characteristics of the SSP scenarios adopted from O'Neil et al. 2017.

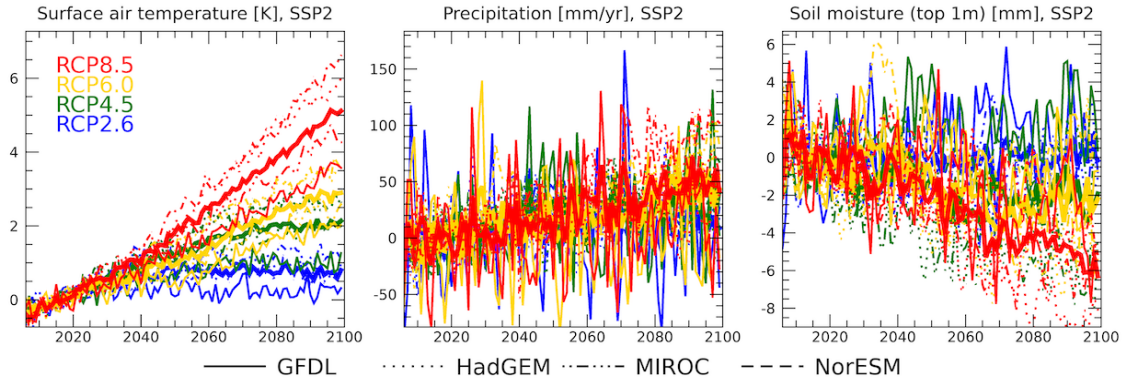


Figure S1. Time sequence of anomalies in surface air temperature (left, unit is K), precipitation (middle, unit is mm/year), and volumetric soil moisture content (right, unit is mm in top 1m). The baseline of anomaly is the 20-year average from 2006-2025. The surface air temperature and precipitation are used as the input for the model, and other variables are calculated by MIROC-INTEG-LAND. Global average (surface air temperature) and average for global land area (precipitation, soil moisture) are shown. The line colors show the results obtained under the RCP2.6 (blue), RCP4.5 (green), RCP6.0 (yellow), and RCP8.5 (red) scenarios. Thin lines are the results obtained from four GCMs, and thick lines are the average values obtained from four GCMs.

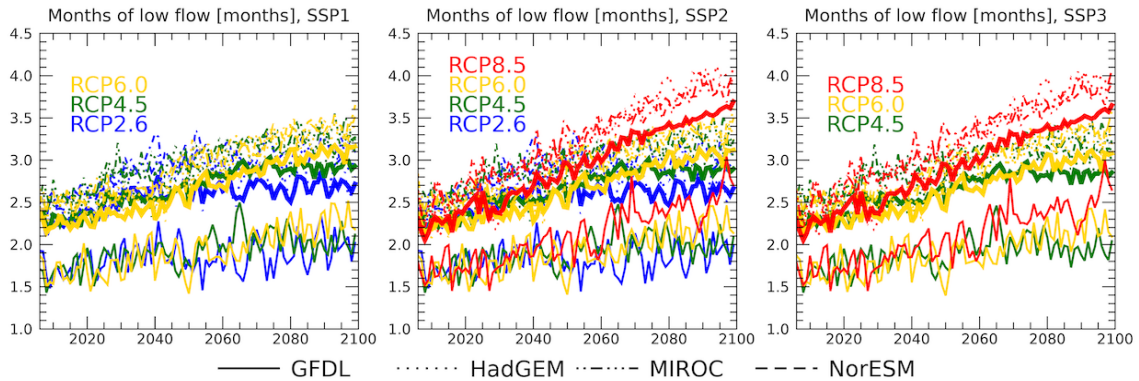


Figure S2. Time sequence of the number of drought months calculated by MIROC-INTEG-LAND. The average results over the global land area are shown. Drought months are defined as the number of months with river flows below the 20 percentiles for each month in historical experiments (1950-2005). If the number of drought months is 3, it means that there are 3 months in the year with river flows below the 20

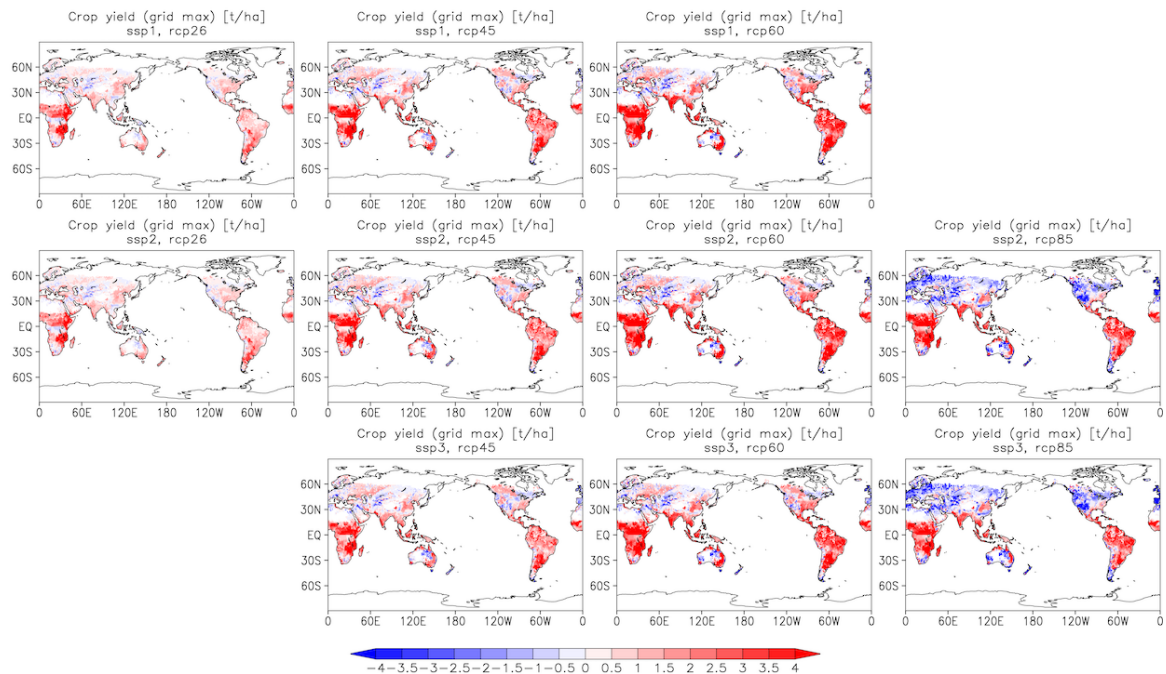


Figure S3. Global map showing anomalies in crop yields (unit is tons/ha). The anomalies are calculated by the difference between the averages of 2081-2100 and 2006-2025. Crop yield is calculated in the same way as in Figure 3.

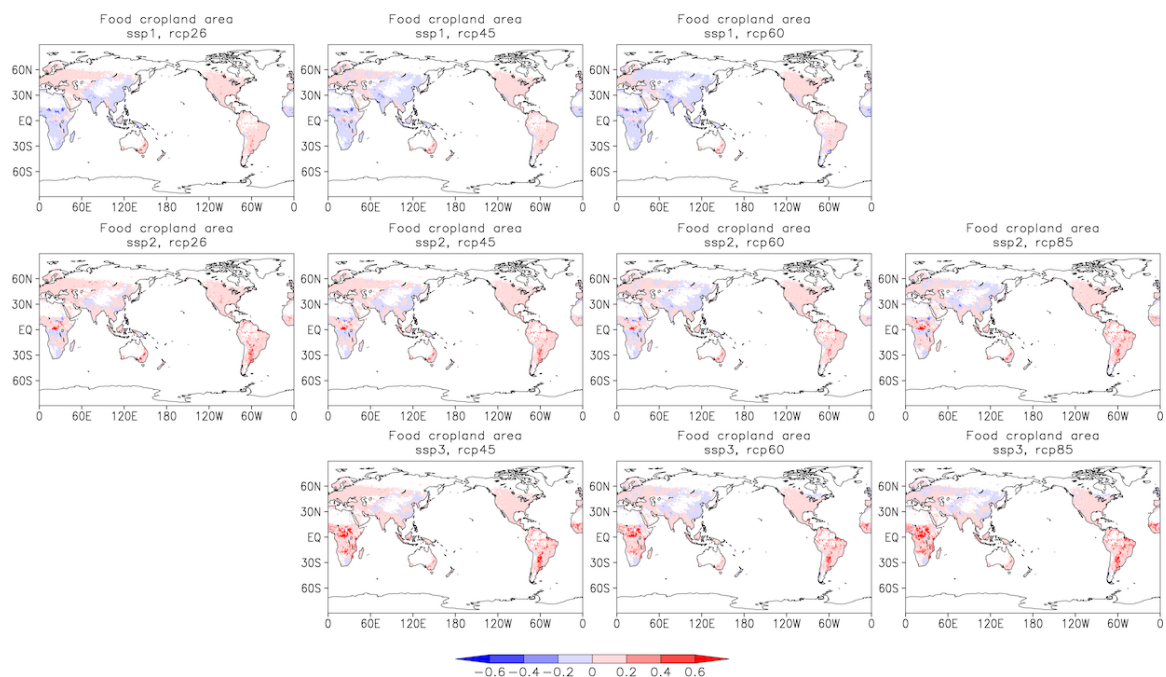


Figure S4. Same as Figure S3, but for anomalies in food cropland area. The unit is the ratio of the cropland area in each grid / total area of the grid.

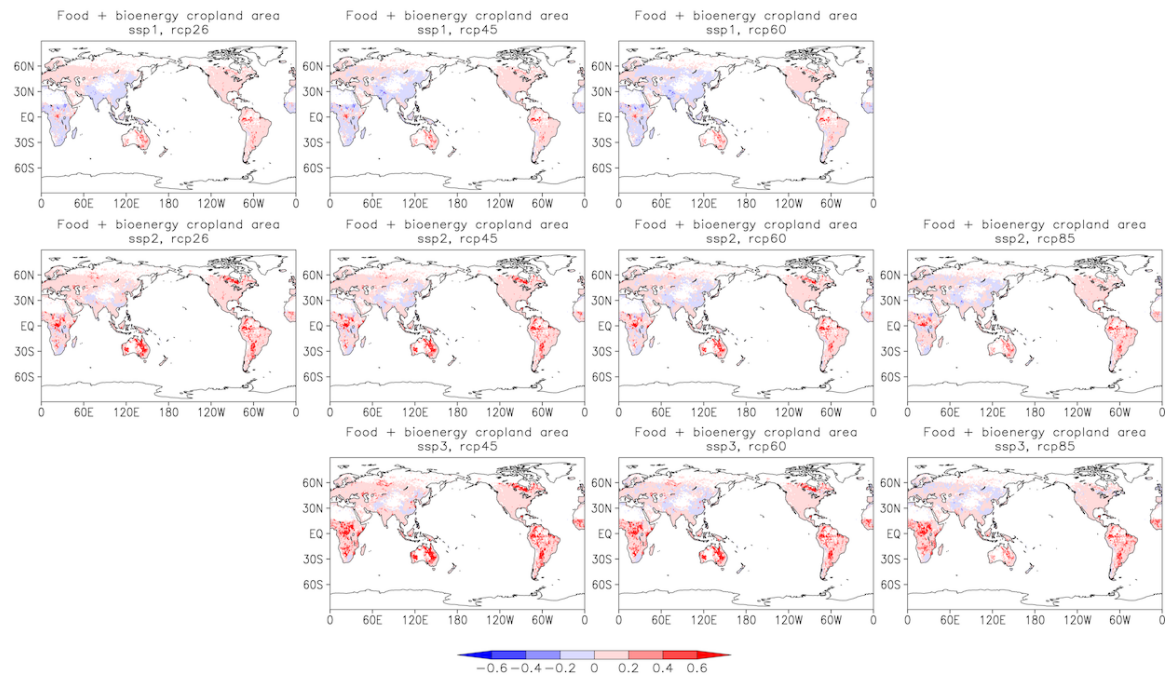


Figure S5. Same as Figure S3, but for anomalies in bioenergy cropland area. The unit is the same as that in Figure S4.

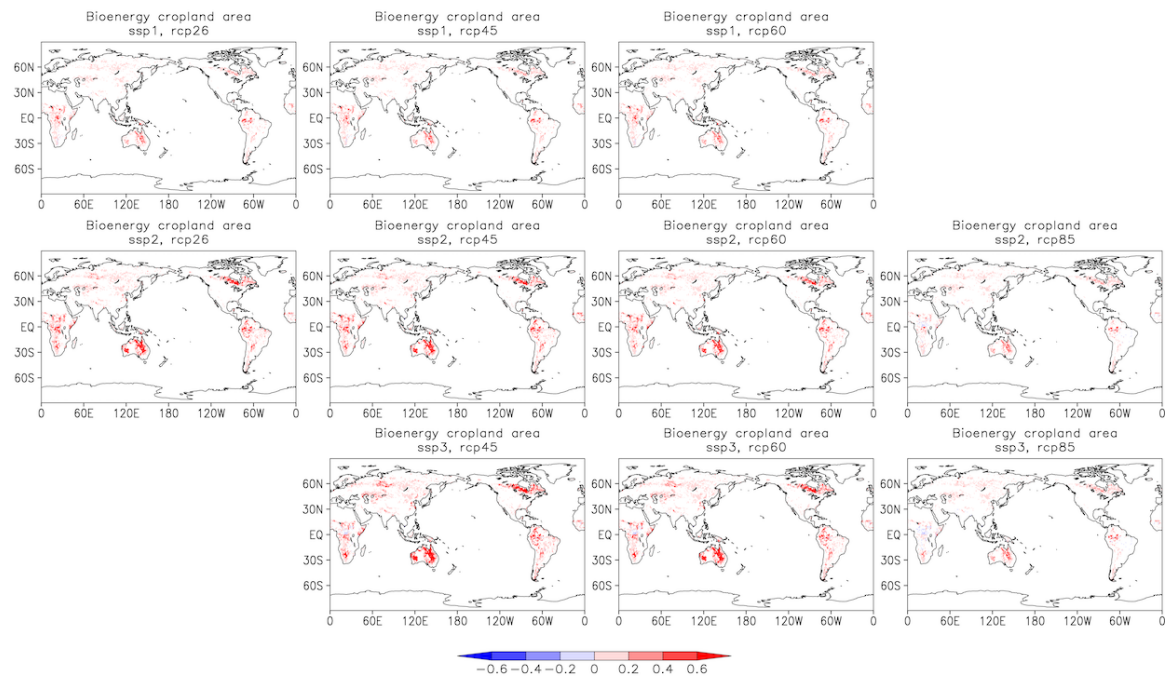


Figure S6. Same as Figure S3, but for anomalies in bioenergy cropland area. The unit is the same as that in Figure S4.

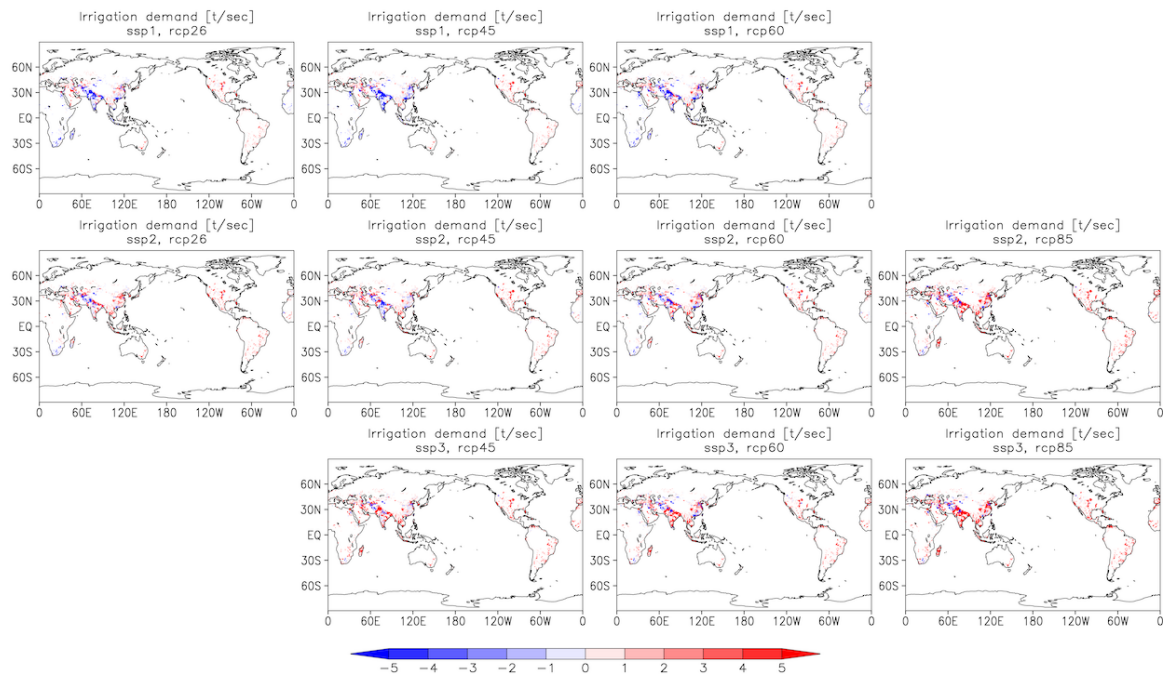


Figure S7. Same as Figure S3, but for anomalies in water demand for irrigation. The unit is kg/sec in each grid (1° longitude and latitude).

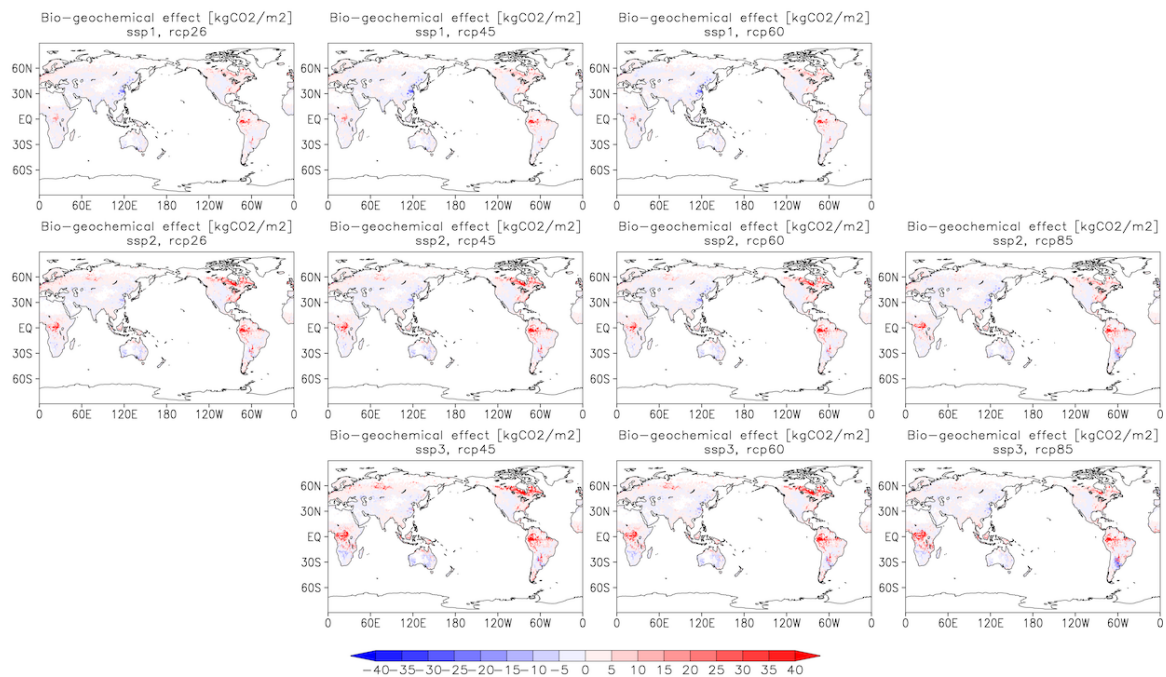


Figure S8. Time Cumulative CO_2 emissions due to land use change. The cumulative emission from 2006 to 2100 is shown. The unit is kgCO_2/m^2 .